

79-1214 748

UNSTEADY WINDINGS ON A SINUOSIDALLY OSCILLATING
 SUPERCRITICAL AIRFOIL(U) NATIONAL AEROSPACE LAB
 AMSTERDAM (NETHERLANDS) N TIJDENNEN JUL 79

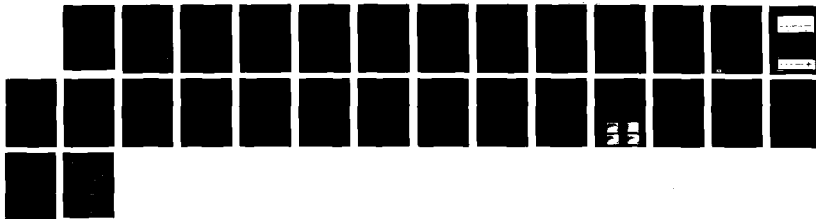
1/2

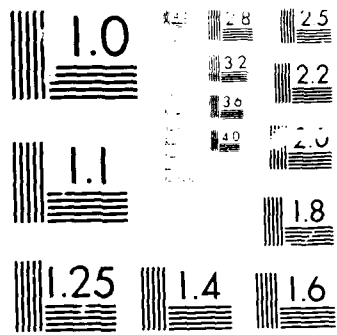
UNCLASSIFIED

NRL-N-NE-79-015 AFOSR-TR-89-1379

F/B 28/4

ML





DTIC FILE COPY

SECURITY CLASSIFICATION OF THIS PAGE

REPORT DOCUMENTATION PAGE

Form Approved
OMB No. 0704-0188

AD-A214 740

1b. RESTRICTIVE MARKINGS

3. DISTRIBUTION/AVAILABILITY OF REPORT
Approved for public release;
distribution unlimited.

4. PERFORMING ORGANIZATION REPORT NUMBER(S)

5. MONITORING ORGANIZATION REPORT NUMBER(S)

AFOSR TR-89-1379

6a. NAME OF PERFORMING ORGANIZATION
National Aerospace Lab
Anthony Fokkerweg 26b. OFFICE SYMBOL
(If applicable)

7a. NAME OF MONITORING ORGANIZATION

AFOSR

6c. ADDRESS (City, State, and ZIP Code)
Amsterdam 1017, Netherlands7b. ADDRESS (City, State, and ZIP Code)
BLDG 410
BAFB DC 20332-64488a. NAME OF FUNDING/SPONSORING
ORGANIZATION

AFOSR

8b. OFFICE SYMBOL
(If applicable)

9. PROCUREMENT INSTRUMENT IDENTIFICATION NUMBER

AFOSR 77-32-3207

8c. ADDRESS (City, State, and ZIP Code)

10. SOURCE OF FUNDING NUMBERS

BLDG 410
BAFB DC 20332-6448PROGRAM
ELEMENT NO.
61102FPROJECT
NO.
2307TASK
NO.
A1WORK UNIT
ACCESSION NO.

11. TITLE (Include Security Classification)

UNSTEADY AIRLOADS ON A SINUSOIDALLY OSCILLATING SUPERCRITICAL AIRFOIL

12. PERSONAL AUTHOR(S)
H. Tijdeman13a. TYPE OF REPORT
Final13b. TIME COVERED
FROM 4/1/77 to 2/31/7814. DATE OF REPORT (Year, Month, Day)
July 197915. PAGE COUNT
3

16. SUPPLEMENTARY NOTATION

17. COSATI CODES

FIELD	GROUP	SUB-GROUP

18. SUBJECT TERMS (Continue on reverse if necessary and identify by block number)

19. ABSTRACT (Continue on reverse if necessary and identify by block number)

DTIC
ELECTE
NOV 28 1989
S B D

20. DISTRIBUTION/AVAILABILITY OF ABSTRACT

☒ UNCLASSIFIED/UNLIMITED ☐ SAME AS RPT ☐ DTIC USERS

21. ABSTRACT SECURITY CLASSIFICATION

unclassified

22a. NAME OF RESPONSIBLE INDIVIDUAL

22b. TELEPHONE (Include Area Code)
767-498722c. OFFICE SYMBOL
NA

11 123

NATIONAAL LUCHT-EN RUIMTEVAARTLABORATORIUM

NATIONAL AEROSPACE LABORATORY NLR THE NETHERLANDS



AFOSR-TR-89-1379

MEMORANDUM AE-79-015

UNSTEADY AIRLOADS ON A SINUSOIDALLY OSCILLATING
SUPERCRITICAL AIRFOIL (FINAL REPORT)

by

H. Tijdeman

This investigation was sponsored by AFOSR under Grant AFOSR-
77-3297 and was monitored by Capt. Donald J. Wilkins

Division : Fl. Dyn.

Prepared : H. Tijdeman

Approved : *ix*

Contractnumber :

NLR order - /codenumber: 20.306

Completed



1 INTRODUCTION

The aim of the proposed investigation was to generate a set of theoretical and experimental unsteady aerodynamic data for an advanced type airfoil. This set of data should serve as a standard for the comparison and the evaluation of computational methods for two-dimensional unsteady transonic flow. For this purpose it was intended to complement the results of the wind tunnel tests conducted at NLR on the supercritical NLR 7301 airfoil with theoretical results to be computed with the method of Dr. R.J. Magnus and Dr. H. Yoshihara* of General Dynamics, San Diego. The calculations, to be performed by General Dynamics, were supposed to be sponsored by the office of Naval Research.

→ The statement of work of the intended investigation was:

- NLR provides the contour data of the "shock-free" NLR 7301 airfoil section, together with the hodograph solution for the design condition.
- NLR provides the measured steady and unsteady pressure distributions in three characteristic flow conditions : subsonic flow, transonic flow with a well developed supercritical region terminated by a shock wave and the "shock-free" design condition.
- General Dynamics performs computations with their "exact" method to obtain theoretical results for the three mentioned flow conditions.
- General Dynamics and NLR will put together the corresponding results in a common report, including a critical evaluation.

Unfortunately, due to lack of sufficient funds to perform the final set of computations the proposed program could not be completed.

This report gives a summary of the work performed so far.

2 EXPERIMENTS

At NLR an extensive wind tunnel investigation has been conducted to explore the unsteady aerodynamic characteristic of so-called supercritical airfoils. In this framework detailed steady and unsteady pressure distributions have been measured on the oscillating 16.5 percent thick NLR 7301 airfoil (for contour data see table 1), which was designed with the hodograph method of Boerstool (Ref. 1).

(*) At present Dr. Yoshihara is employed by the Boeing Co.

<input checked="checked" type="checkbox"/>
<input type="checkbox"/>
<input type="checkbox"/>
Codes
1/or
Special
A-1



Emphasis was put on three mean flow conditions, which can be characterized as follows :

- A : subsonic flow
- B : transonic flow with a well developed supersonic region on the upper surface terminated by a relatively strong shock wave
- C : the "shock-free" design condition.

According to the statement of work, the contour data and the test results were made available to General Dynamics. Further, independently of the present investigation, the results of the experiments, including a thorough analysis, have been presented during the AGARD conference on "unsteady airloads in separated and transonic flow", Lisbon, April 1977. For convenience of the reader, a reprint of the AGARD paper is added to this report as Appendix A.

Meanwhile, the NLR 7301 airfoil has been selected as one of the test cases for the AGARD activity "Standard Aeroelastic Configurations". For that purpose all relevant data (geometry description, aerodynamic conditions and tabulated experimental values) have been gathered in tabular form in reference 2.

3 COMPUTATIONS

As stated earlier, it was intended to complement the results of the experiments with results obtained with the computational method developed by Magnus and Yoshihara (Refs. 3. 4). Their method, which can be considered as one of the most advanced methods at present available for unsteady flow computations, solves the Euler equations without further assumptions concerning frequency or amplitude of oscillation. The boundary conditions are imposed along a contour coincident with the mean position of the airfoil. The computations start with the steady flow solution and are continued until a complete cycle of the periodic flow is obtained. This is a time-consuming process and therefore the method is not suited for routine use, but rather to generate some solutions that might reveal the nature of the flow or serve as test cases for more approximative but faster methods.

Dr. Magnus performed a set of computations for the NLR 7301 airfoil and gathered the results in report CASD/LVP 78-013 entitled "Some numerical solutions of inviscid, unsteady transonic flow over the NLR 7301 airfoil" (Ref. 5). His results showed many of the features of the experiments, but that there were differences due to the effect of the tunnel walls, the presence of the boundary layer and the fact that in the calculated results insufficient expansion of the



flow along the upper part of the nose could be obtained (Fig. 1). Further it was experienced that the final result was influenced considerably when in the computations the trailing edge was chopped.

In view of these results it was decided that the present study could only be finished in a fruitful way if the following additional calculations were performed :

condition	M	geometric incidence α_o	incidence corrected for wall interference α_c	reduced frequency $k = \frac{\omega C}{2U}$	
A1	0.5	(0.85°)	0.40°	0.263	With tail
B1	0.7	(3.00°)	2.00°	0.192	
C1	0.721	-	-0.19°	0.181	
condition	M	α_o	α_c	k	
B	0.7	(3.00°)	2.00°	0.192	tail chopped at x = 1.00
C	0.721	-	- 0.19°	0.181	

The amplitude of oscillation around the pitch axis at 40 percent chord amounts 0.5°

Essential is that the computations were to be performed for mean incidences α_o in which the effect of the tunnel walls is taken into account. In this way it is assured that in the calculations oscillatory perturbations around the same mean steady flow field are considered as occurred in the experiments.

As far as the "shock-free" flow condition is concerned, preference is given to the theoretical design condition, which is found at $M = 0.721$ and $\alpha = - .19^\circ$

Unfortunately, the computations for the cases summarized in the foregoing table could not be performed, since no funds could be made available to Dr. Magnus to make the additional computer runs.



4 CONCLUDING REMARKS

Due to the fact that the final set of computations cannot be performed, also the remaining tasks for NLR, namely a comparison between theory and experiment and a critical evaluation of the results in collaboration with General Dynamics cannot be completed. The AFOSR funds which were made available for this part of the NLR work will be returned to AFOSR.

5 REFERENCES

- 1 Boerstel, W.J. Design and analysis of a hodograph method for the calculation of supercritical shock-free aerofoils.
NLR TR 77046 U, 1977.
- 2 Zwaan, R.J. Summary of data required for the AGARD SMP activity "Standard Aeroelastic Configurations" - Two Dimensional Configurations. NLR MP 79015 U, 1979.
- 3 Magnus, R.J. Finite difference calculations of the
Yoshihara, H. NACA 64A-410 airfoil oscillating sinusoidally in pitch at $M_\infty = 0.72$ Convair report NSC-74-004, 1974.
- 4 Magnus, R.J. Calculations of transonic flow over an
Yoshihara, H. oscillating airfoil.
AIAA paper 75-98; 13 th Aerospace Sciences Meeting, Pasadena, Jan. 1975.
- 5 Magnus, R.J. Some numerical solutions of inviscid, unsteady, transonic flows over the NLR 7301 airfoil.
CASD/LVP 78-013, Jan 1978.



TABLE 1

Contour data of airfoil NLR 7301

UPPER PART				LOWER PART			
X/C	Z/C	X/C	Z/C	X/C	Z/C	X/C	Z/C
0.0000012	-0.0004162	0.4297667	-0.0000136	0.0000012	-0.0004162	0.4297667	-0.0000136
0.0002895	-0.0052191	0.4346044	-0.0004447	0.0002895	-0.0052191	0.4346044	-0.0004447
0.0005870	-0.0074744	0.4467642	-0.0007644	0.0005870	-0.0074744	0.4467642	-0.0007644
0.0008861	-0.0095945	0.4642811	-0.0009475	0.0008861	-0.0095945	0.4642811	-0.0009475
0.0011754	-0.0112217	0.4861193	-0.0012236	0.0011754	-0.0112217	0.4861193	-0.0012236
0.0014662	-0.0124337	0.5120011	-0.0014509	0.0014662	-0.0124337	0.5120011	-0.0014509
0.0017465	-0.0138916	0.5418073	-0.0017271	0.0017465	-0.0138916	0.5418073	-0.0017271
0.0020217	-0.0150411	0.5746043	-0.0020037	0.0020217	-0.0150411	0.5746043	-0.0020037
0.0022989	-0.0160874	0.6100070	-0.0022803	0.0022989	-0.0160874	0.6100070	-0.0022803
0.0025701	-0.0170734	0.6476013	-0.0025569	0.0025701	-0.0170734	0.6476013	-0.0025569
0.0028314	-0.0179874	0.6870070	-0.0028335	0.0028314	-0.0179874	0.6870070	-0.0028335
0.0030820	-0.0188204	0.7280070	-0.0031101	0.0030820	-0.0188204	0.7280070	-0.0031101
0.0033212	-0.0195817	0.7700070	-0.0033867	0.0033212	-0.0195817	0.7700070	-0.0033867
0.0035493	-0.0202824	0.8130070	-0.0036633	0.0035493	-0.0202824	0.8130070	-0.0036633
0.0037664	-0.0209237	0.8570070	-0.0039400	0.0037664	-0.0209237	0.8570070	-0.0039400
0.0039725	-0.0215050	0.9020070	-0.0042166	0.0039725	-0.0215050	0.9020070	-0.0042166
0.0041676	-0.0220273	0.9480070	-0.0044933	0.0041676	-0.0220273	0.9480070	-0.0044933
0.0043517	-0.0224906	0.9950070	-0.0047699	0.0043517	-0.0224906	0.9950070	-0.0047699
0.0045248	-0.0228949	1.0430070	-0.0050466	0.0045248	-0.0228949	1.0430070	-0.0050466
0.0046869	-0.0232402	1.0920070	-0.0053232	0.0046869	-0.0232402	1.0920070	-0.0053232
0.0048380	-0.0235265	1.1420070	-0.0056000	0.0048380	-0.0235265	1.1420070	-0.0056000
0.0049791	-0.0237538	1.1930070	-0.0058767	0.0049791	-0.0237538	1.1930070	-0.0058767
0.0051102	-0.0239211	1.2450070	-0.0061534	0.0051102	-0.0239211	1.2450070	-0.0061534
0.0052313	-0.0240384	1.2980070	-0.0064301	0.0052313	-0.0240384	1.2980070	-0.0064301
0.0053424	-0.0241057	1.3520070	-0.0067068	0.0053424	-0.0241057	1.3520070	-0.0067068
0.0054435	-0.0241330	1.4070070	-0.0069835	0.0054435	-0.0241330	1.4070070	-0.0069835
0.0055346	-0.0241203	1.4630070	-0.0072602	0.0055346	-0.0241203	1.4630070	-0.0072602
0.0056157	-0.0240776	1.5200070	-0.0075369	0.0056157	-0.0240776	1.5200070	-0.0075369
0.0056868	-0.0240049	1.5780070	-0.0078136	0.0056868	-0.0240049	1.5780070	-0.0078136
0.0057479	-0.0239022	1.6370070	-0.0080903	0.0057479	-0.0239022	1.6370070	-0.0080903
0.0057990	-0.0237695	1.6970070	-0.0083670	0.0057990	-0.0237695	1.6970070	-0.0083670
0.0058401	-0.0236068	1.7580070	-0.0086437	0.0058401	-0.0236068	1.7580070	-0.0086437
0.0058712	-0.0234141	1.8200070	-0.0089204	0.0058712	-0.0234141	1.8200070	-0.0089204
0.0058923	-0.0231914	1.8830070	-0.0091971	0.0058923	-0.0231914	1.8830070	-0.0091971
0.0059034	-0.0229387	1.9470070	-0.0094738	0.0059034	-0.0229387	1.9470070	-0.0094738
0.0059045	-0.0226560	2.0120070	-0.0097505	0.0059045	-0.0226560	2.0120070	-0.0097505
0.0058956	-0.0223433	2.0780070	-0.0100272	0.0058956	-0.0223433	2.0780070	-0.0100272
0.0058767	-0.0220006	2.1450070	-0.0103039	0.0058767	-0.0220006	2.1450070	-0.0103039
0.0058478	-0.0216279	2.2130070	-0.0105806	0.0058478	-0.0216279	2.2130070	-0.0105806
0.0058089	-0.0212252	2.2820070	-0.0108573	0.0058089	-0.0212252	2.2820070	-0.0108573
0.0057600	-0.0207925	2.3520070	-0.0111340	0.0057600	-0.0207925	2.3520070	-0.0111340
0.0057011	-0.0203298	2.4230070	-0.0114107	0.0057011	-0.0203298	2.4230070	-0.0114107
0.0056322	-0.0198371	2.4950070	-0.0116874	0.0056322	-0.0198371	2.4950070	-0.0116874
0.0055533	-0.0193144	2.5680070	-0.0119641	0.0055533	-0.0193144	2.5680070	-0.0119641
0.0054644	-0.0187717	2.6420070	-0.0122408	0.0054644	-0.0187717	2.6420070	-0.0122408
0.0053655	-0.0182090	2.7170070	-0.0125175	0.0053655	-0.0182090	2.7170070	-0.0125175
0.0052566	-0.0176263	2.7930070	-0.0127942	0.0052566	-0.0176263	2.7930070	-0.0127942
0.0051377	-0.0170236	2.8700070	-0.0130709	0.0051377	-0.0170236	2.8700070	-0.0130709
0.0050088	-0.0164009	2.9480070	-0.0133476	0.0050088	-0.0164009	2.9480070	-0.0133476
0.0048700	-0.0157582	3.0270070	-0.0136243	0.0048700	-0.0157582	3.0270070	-0.0136243
0.0047211	-0.0150955	3.1070070	-0.0139010	0.0047211	-0.0150955	3.1070070	-0.0139010
0.0045623	-0.0144128	3.1880070	-0.0141777	0.0045623	-0.0144128	3.1880070	-0.0141777
0.0043934	-0.0137101	3.2700070	-0.0144544	0.0043934	-0.0137101	3.2700070	-0.0144544
0.0042145	-0.0129874	3.3530070	-0.0147311	0.0042145	-0.0129874	3.3530070	-0.0147311
0.0040256	-0.0122447	3.4370070	-0.0150078	0.0040256	-0.0122447	3.4370070	-0.0150078
0.0038267	-0.0114820	3.5220070	-0.0152845	0.0038267	-0.0114820	3.5220070	-0.0152845
0.0036178	-0.0107093	3.6080070	-0.0155612	0.0036178	-0.0107093	3.6080070	-0.0155612
0.0033989	-0.0100266	3.6950070	-0.0158379	0.0033989	-0.0100266	3.6950070	-0.0158379
0.0031700	-0.0093339	3.7830070	-0.0161146	0.0031700	-0.0093339	3.7830070	-0.0161146
0.0029311	-0.0086312	3.8720070	-0.0163913	0.0029311	-0.0086312	3.8720070	-0.0163913
0.0026822	-0.0079185	3.9620070	-0.0166680	0.0026822	-0.0079185	3.9620070	-0.0166680
0.0024233	-0.0071958	4.0530070	-0.0169447	0.0024233	-0.0071958	4.0530070	-0.0169447
0.0021544	-0.0064631	4.1450070	-0.0172214	0.0021544	-0.0064631	4.1450070	-0.0172214
0.0018755	-0.0057204	4.2380070	-0.0174981	0.0018755	-0.0057204	4.2380070	-0.0174981
0.0015866	-0.0049777	4.3320070	-0.0177748	0.0015866	-0.0049777	4.3320070	-0.0177748
0.0012877	-0.0042350	4.4270070	-0.0180515	0.0012877	-0.0042350	4.4270070	-0.0180515
0.0009788	-0.0034923	4.5230070	-0.0183282	0.0009788	-0.0034923	4.5230070	-0.0183282
0.0006600	-0.0027496	4.6200070	-0.0186049	0.0006600	-0.0027496	4.6200070	-0.0186049
0.0003311	-0.0020069	4.7180070	-0.0188816	0.0003311	-0.0020069	4.7180070	-0.0188816
0.0000022	-0.0012642	4.8170070	-0.0191583	0.0000022	-0.0012642	4.8170070	-0.0191583
		4.9170070	-0.0194350			4.9170070	-0.0194350
		5.0180070	-0.0197117			5.0180070	-0.0197117
		5.1200070	-0.0200000			5.1200070	-0.0200000
		5.2230070	-0.0202883			5.2230070	-0.0202883
		5.3270070	-0.0205766			5.3270070	-0.0205766
		5.4320070	-0.0208649			5.4320070	-0.0208649
		5.5380070	-0.0211532			5.5380070	-0.0211532
		5.6450070	-0.0214415			5.6450070	-0.0214415
		5.7530070	-0.0217298			5.7530070	-0.0217298
		5.8620070	-0.0220181			5.8620070	-0.0220181
		5.9720070	-0.0223064			5.9720070	-0.0223064
		6.0830070	-0.0225947			6.0830070	-0.0225947
		6.1950070	-0.0228830			6.1950070	-0.0228830
		6.3080070	-0.0231713			6.3080070	-0.0231713
		6.4220070	-0.0234596			6.4220070	-0.0234596
		6.5370070	-0.0237479			6.5370070	-0.0237479
		6.6530070	-0.0240362			6.6530070	-0.0240362
		6.7700070	-0.0243245			6.7700070	-0.0243245
		6.8880070	-0.0246128			6.8880070	-0.0246128
		7.0070070	-0.0249011			7.0070070	-0.0249011
		7.1270070	-0.0251894			7.1270070	-0.0251894
		7.2480070	-0.0254777			7.2480070	-0.0254777
		7.3700070	-0.0257660			7.3700070	-0.0257660
		7.4930070	-0.0260543			7.4930070	-0.0260543
		7.6170070	-0.0263426			7.6170070	-0.0263426
		7.7420070	-0.0266309			7.7420070	-0.0266309
		7.8680070	-0.0269192			7.8680070	-0.0269192
		7.9950070	-0.0272075			7.9950070	-0.0272075
		8.1230070	-0.0274958			8.1230070	-0.0274958
		8.2520070	-0.0277841			8.2520070	-0.0277841
		8.3820070	-0.0280724			8.3820070	-0.0280724
		8.5130070	-0.0283607			8.5130070	-0.0283607
		8.6450070	-0.0286490			8.6450070	-0.0286490
		8.7780070	-0.0289373			8.7780070	-0.0289373
		8.9120070	-0.0292256			8.9120070	-0.0292256
		9.0470070	-0.0295139			9.0470070	-0.0295139
		9.1830070	-0.0298022			9.1830070	-0.0298022
		9.3200070	-0.0300905			9.3200070	-0.0300905
		9.4580070	-0.0303788			9.4580070	-0.0303788
		9.5970070	-0.0306671			9.5970070	-0.0306671
		9.7370070	-0.0309554			9.7370070	-0.0309554
		9.8780070	-0.0312437			9.8780070	-0.0312437
		10.0200070	-0.0315320			10.0200070	-0.0315320
		10.1630070	-0.0318203			10.1630070	-0.0318203
		10.3070070	-0.0321086			10.3070070	-0.0321086
		10.4520070	-0.0323969			10.4520070	-0.0323969
		10.5980070	-0.0326852			10.5980070	-0.0326852
		10.7450070	-0.0329735			10.7450070	-0.0329735
		10.8930070	-0.0332618			10.8930070	-0.0332618
		11.0420070	-0.0335501			11.0420070	-0.0335501
		11.1920070	-0.0338384			11.1920070	-0.0338384
		11.3430070	-0.0341267			11.3430	

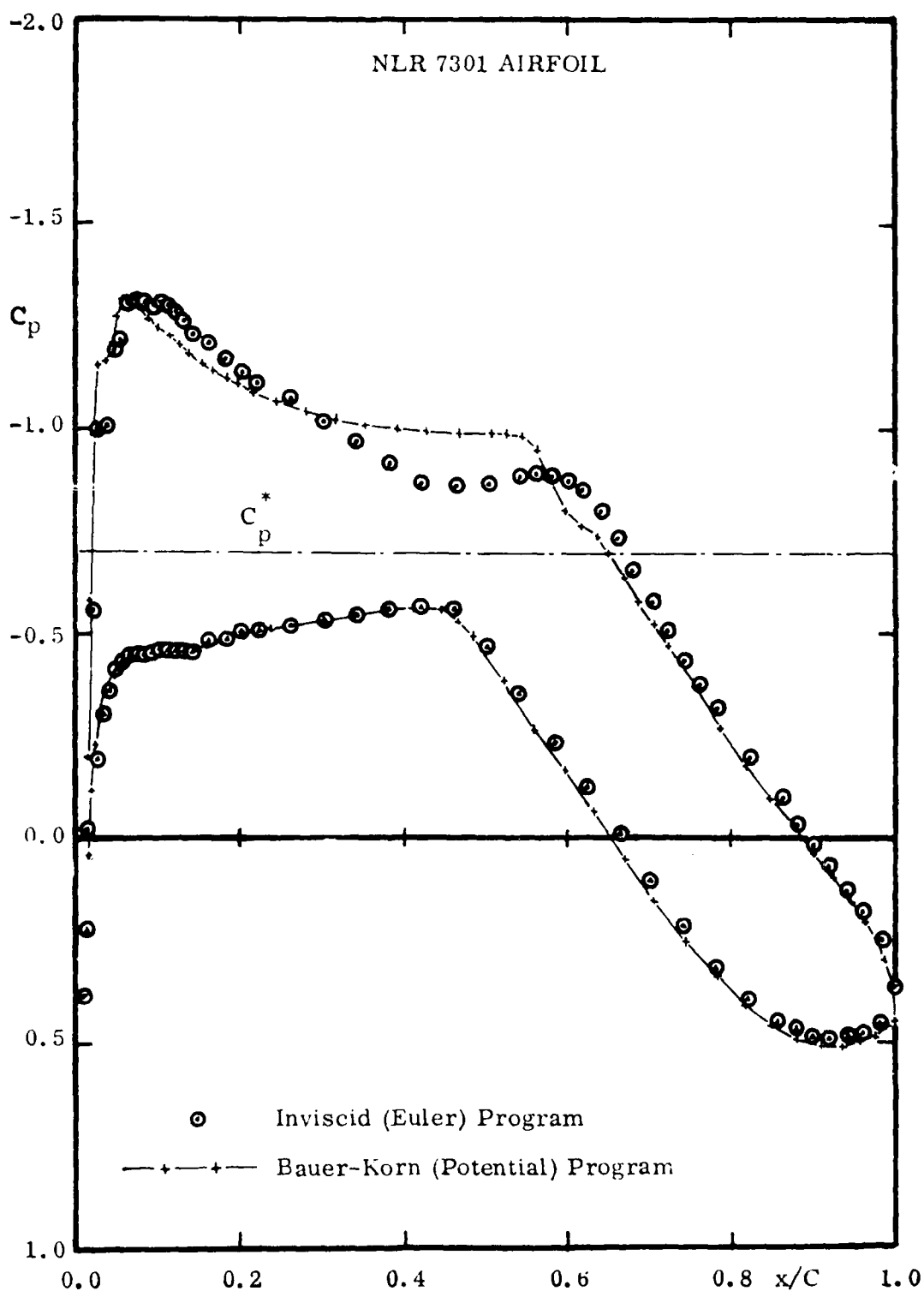


Fig. 1 Calculated pressure distribution, Mach 0.721,
 $\alpha = 0.00^\circ$, unrestricted stream (Ref.5)

NATIONAAL LUCHT- EN RUIMTEVAAR. LABORATORIUM National Aerospace Laboratory NLR



Anthony Fokkerweg 2 Amsterdam-1017 Nederland

AFOSR-TR. 80-0093

All communications should be addressed to
the Director. In your reply please quote date
and number.

Capt. Donald J. Wilkins
AFOSR-TKN Building 410
Bolling AFB
Washington DC 20332
U.S.A.

Subject:
Grant AFOSR-77-3297

Orderno. 20.302

Your Ref.

Your letter:

Our Ref.

A/3582

Date

5 JUL

Encl.: 4

Dear Capt. Wilkins,

Thank you for your letter of June 19th, dealing with the AFOSR Grant
"Unsteady airloads on a sinusoidally oscillating supercritical air-
foil", which expired on Dec. 31st., 1978.

As you know, the aim of the proposed investigation was to generate a
set of unsteady aerodynamic data for an advanced type of airfoil,
both theoretical and experimental, which may serve as a standard for
comparison and evaluation of calculation methods for two-dimensional
unsteady transonic flow. For this purpose, it was intended to comple-
ment the results of the wind tunnel tests conducted at the NLR on the
16.5 percent thick NLR 7301 airfoil with calculated results obtained
with the method of Dr. Richard J. Magnus and Dr. H. Joshikara of
General Dynamics San Diego. In collaboration with General Dynamics
a comparison and critical evaluation should be made of both theory
and experiment.

The calculations to be performed by General Dynamics were supposed
to be sponsored by the Office of Naval Research.

NLR provided the contour data of the airfoil and the relevant test
data to General Dynamics. Further, apart from the present investiga-
tion, an analysis of the test results was presented during the AGARD
Conference on "Unsteady airloads in separated and transonic flow",
Lisbon, April 1977 (see Agard CP 226). Moreover, details of the ex-
periments and its results have been published in NLR report TR 77090 U:
"Investigations of the transonic flow past oscillating airfoils".

Meanwhile, Dr. Magnus performed a first set of calculations on the
NLR 7301 airfoil and sent us some results with his letter of 12 Jan.
1978 (see enclosure A). This set of results has been published in

The foundation NLR does not accept financial liability ensuing from its advices.

NATIONAL - LUCHT- EN RUIMTEVAARTIG ORATORIUM
National Aerospace Laboratory NLR

Geadresseerde
Addressee

Capt. Donald J. Wilkins

Org. kenmerk
Org. ref

A/3337

Datum
Date

5 JUL 1979

Bladnr.
Page

2

././ report CASD/LWF 78-111 entitled "Some numerical solutions of inviscid, unsteady, transonic flows over the NLR 7301 airfoil" by R.J. Magnus (1978). The letter of Dr. Magnus (enclosure A) gives a resumé of the unforeseen problems he encountered during the computations and his financial problems in continuing the work.

././ In our letter of April 11 th (enclosure B), we gave some comments on the results computed so far and indicated that in order to continue our part of the investigations in a fruitful way, some additional calculations were required.

These calculations were discussed in detail between Dr. Magnus, Dr. Tijdeman, and Dr. Sanford Davis of NASA during the workshop on transonic aerodynamics for aeroelastic applications (Columbus, Ohio, Nov. 1978). Agreement was reached on the specific calculations still to be performed. An interesting aspect, brought up by Dr. Magnus, was the sensitivity of the results to the cut-off of the trailing edge and it was decided also to add some calculations to reveal this effect.

././ The final program was confirmed in our letter of 11 Jan. 1979 (see enclosure C) and, in order to avoid any misunderstanding, a set of the airfoil contour data was enclosed again.

././ From the letter we received from Dr. Davis (see enclosure D) we learned that no funds could be provided to perform the final set of calculations by Dr. Magnus.

In view of this development it is not possible for us to finish the work as originally planned. For this reason we ask you formal permission to stop the work under the Grant. If you agree we will write a brief scientific report and send it to major Howell at EOARD together with a final invention report and a final fiscal report as soon as possible. A check for the unspent grant funds will be sent directly to your office.

In our opinion it is a pity that the work cannot be completed. We discussed this with Dr. Sanford Davis (NASA) and Mr. Charles F. Coe (NASA) and they feel the same. During a visit of Mr. Coe at NLR last June we discussed the following aspects:

- Dr. Chyu of NASA Ames is able to perform similar computations for the NLR 7301 airfoil as originally planned by Dr. Magnus. The computer program of Dr. Chyu, however, is much faster.
- NASA Ames has performed an experimental program on the oscillating NLR 7301 airfoil in their 11 ft. transonic windtunnel putting emphasis on the effect of Reynolds number, amplitude of oscillating and mode of vibration.

NATIONA LUCHT- EN RUIMTEVAARTL ORATORIUM
National Aerospace Laboratory NLR

Gedresseerde
Addressee

Capt. Donald J. Wilkins

Ges. nummer
Our ref

A/5507

Datum
Date

5 JUL 1979

B. adnr
Page

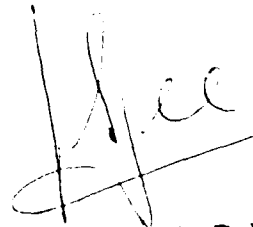
3

In principle this offers an excellent opportunity to generate an interesting set of data for the NLR T101 aircraft, consisting of two sets of measurements and calculations with the help of the Euler equations.

We spoke about the possibility that Dr. Davis and Dr. Tildeman could write a common report on the NASA and NLR experiments and the calculations. Their paper a.o. should contain a critical review of the comparison between theory and experiment.

Mr. Joe and Dr. Davis will discuss this in more detail after Mr. Coe's return to the U.S. (July 8th). If this leads to a real possibility to continue the work, we will address ourselves to your office with a new proposal for financial support of AFOSR.

Sincerely yours,
Nationaal Lucht- en Ruimtevaartlaboratorium
(National Aerospace Laboratory NLR)



Dr. Ir. B. M. SPEE
Adj. Directeur

Opz. van T101 met 1. en 2.
NASA/Dr. Davis
AFOSR/Dr. Coe

HT/EC

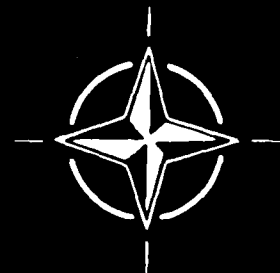
AGARD

ADVISORY GROUP FOR AEROSPACE RESEARCH & DEVELOPMENT

7 RUE ANCELLE 92200 NEUILLY SUR SEINE FRANCE

Paper Reprinted from
Conference Proceedings No.226
Unsteady Airloads in
Separated and Transonic Flow

NORTH ATLANTIC TREATY ORGANIZATION



UNSTEADY AIRLOADS ON AN OSCILLATING SUPERCRITICAL AIRFOIL

by

H. Tijleman, P. Schippers and A.J. Persoon
National Aerospace Laboratory NLR
Anthony Eekkerweg 6, Amsterdam,
The Netherlands

SUMMARY

Results are presented of unsteady pressure measurements on a two-dimensional model of the supercritical NLR 7301 airfoil performing pitching oscillations about an axis at 60 per cent of the chord.

CONTENTS

LIST OF SYMBOLS

1. INTRODUCTION
2. MODEL AND TEST SET-UP
 - 2.1 Model and excitation system
 - 2.2 Optical flow studies
 - 2.3 Wind tunnel
3. ANALYSIS OF RESULTS
 - 3.1 Introductory remarks
 - 3.2 Unsteady pressure distributions
 - 3.2.1 Fully subsonic flow (condition A)
 - 3.2.2 Transonic flow with shock wave (condition B)
 - 3.2.3 The "shock-free" design condition (condition C)
 - 3.3 Unsteady aerodynamic derivatives
 - 3.4 Remarks on the unsteady shock wave motion
 - 3.4.1 Effect of frequency
 - 3.4.2 Linearity of the unsteady loads
4. Expected capability of the new calculation methods
 - 4.1 Fully subsonic flow (condition A)
 - 4.2 Transonic flow with shock wave (condition B)
 - 4.3 The "shock-free" design condition (condition C)
5. CONCLUDING REMARKS
6. ACKNOWLEDGEMENT
7. REFERENCES
 - 1 Table
 - 27 Figures
 - 23 References

LIST OF SYMBOLS

a	velocity of sound
c	chord
C_l	lift coefficient
C_p	steady pressure coefficient
$\Delta C_p = \frac{\Delta p}{\frac{1}{2} \rho U^2}$	unsteady pressure coefficient
f	frequency of oscillation (Hz)
im	component of unsteady pressure in quadrature with the airfoil motion
$k = \frac{\omega}{2c}$	reduced frequency
k_n	unsteady normal force derivative
m_n	unsteady moment derivative about the 1/4-chord point
M	Mach number
p	pressure
Δp	variation in pressure due to variation in incidence
q	dynamic pressure
Re	Reynolds number based on the chord
Re	component of unsteady pressure in phase with the airfoil motion
t	time
t	thickness of airfoil
U	flow velocity
α_0	geometric incidence
α_c	effective incidence (including tunnel wall correction)
α_m	amplitude of the airfoil motion

1. INTRODUCTION

Nowadays there is a considerable interest in methods to predict the unsteady airloads on airfoils and wings oscillating in transonic flow, especially in connection with the current interest in the so-called supercritical wing concept. However, in contrast with the steady flow case, experimental data, that are sufficiently detailed to verify fundamental theoretical assumptions or to confirm the validity of calculated results are very scarce and thus a definite need exists.

For this reason recently at NLR an exploratory wind tunnel investigation has been performed on a model of an oscillating supercritical airfoil, of which the geometry has been generated with the hodograph method of Boerstool (Refs. 1, 2). While the airfoil was oscillating in pitch about an axis at 40 per cent of the chord detailed pressure distributions were determined. In addition time histories of shock wave motions were recorded.

The aim of the present paper is to illustrate some typical high subsonic and transonic effects as observed in the experiments. After a brief description of the test set up, an analysis is given of the pressure distributions and the resulting unsteady airloads as measured for some characteristic flow conditions. Further attention is paid to the periodical motions of the shock wave and finally it is tried to assess what can be expected from the new generation of calculation methods for unsteady transonic flow (For details about the various theoretical methods reference is made to the other papers presented during this meeting).

2. MODEL AND TEST SET UP

2.1 Model and excitation system

The airfoil under consideration, the NLR 7301, was designed for "shock-free" flow under prescribed conditions (Fig. 1) and was tested extensively in steady flow by Rohne and Zwaaneveld (Refs. 3, 4). For the purpose of the present unsteady experiments a new model has been built, which could perform pitching oscillations about an axis at 40 per cent of the chord. This model, made of Dural, has a chord length of 18 cm and spans horizontally the test section of the NLR Pilot tunnel. The pitching motion is generated by means of a hydraulic actuator (For a detailed description of the hydraulic system and the model suspension reference is made to Foestkoke (Ref. 5)). To keep the suspension as simple as possible the model is excited at one side, while the opposite side is supported by a bearing just outside the tunnel wall (Fig. 2). To avoid a complicated sealing between model and window, the window closest to the actuator is attached to the model and follows its motion. In addition it results in a clear view on the model surface for the optical flow studies.

Both the upper and lower surface of the model are provided with 20 pressure orifices (Fig. 3), connected with two scanning valves outside the wind tunnel via pressure tubes. In addition 10 miniature Kulite transducers are built in. This number, which is larger than necessary for the dynamic calibration of the pressure tubes, was chosen to create the possibility to arrest the actual time histories (including the higher harmonics) of the chordwise pressure distribution along the upper surface.

To determine the motion of the model use is made of 6 accelerometers, located in three spanwise sections. The mean incidence is controlled by the hydraulic system.

2.2 Optical flow studies

The periodical shock wave motions on the oscillating model were determined from a series of subsequent shadowgraph pictures. These pictures were taken using a stroboscopic light source, triggered by an electrical signal from a displacement pick up. By means of an adjustable phase shift in the electric circuit between the accelerometer and the light source the oscillating model with its instantaneous shock pattern could be photographed in every position desired.

2.3 Wind tunnel

The experiments were performed in the Pilot tunnel of NLR, which is an atmospheric closed circuit tunnel for Mach numbers up to 1. Upper and lower surface of the test section (height: 55 cm; width: 42 cm) are fitted with longitudinal slotted walls. The open area ratio of the walls is 0.1 and the plenum chambers of floor and bottom are not connected. Further details of the Pilot tunnel can be found in reference 6.

3. ANALYSIS OF RESULTS

3.1 Introductory remarks

The main unsteady aerodynamic characteristics of the NLR 7301 airfoil will be discussed using experimental data for three different flow conditions, which can be characterized as follows (see figure 4):

- A: fully subsonic flow
- B: transonic flow with a well developed shock wave
- C: "shock-free" flow

To emphasize the importance of the dynamic effects on the unsteady airloads, for each case the corresponding quasi-steady airloads will be considered first. These quasi-steady airloads can be interpreted as the airloads when the oscillations were taking place infinitely slow. For reference purposes the experimental results will be compared also with results of the thin airfoil theory.

The unsteady pressures are given in terms of the dimensionless coefficients ΔC_p , defined as

$$\Delta C_p = \frac{\Delta p}{\frac{1}{2} \rho U^2}$$

where Δp is the amplitude of the pitching oscillation in radians, p the pressure variation and $\frac{1}{2} \rho U^2$ the dynamic pressure. The corresponding quasi-steady coefficient can be derived from steady tests at two different incidence as follows:

$$\Delta C_p = \frac{C_p(\alpha_1 + \Delta\alpha) - C_p(\alpha_1 - \Delta\alpha)}{2\Delta\alpha}$$

3.2.1 Unsteady pressure distribution on 3.2.1 Fully supersonic flow (condition A)

The steady pressure distributions measured in supersonic flow (condition A) for two values of the angle of attack and the quasi-steady results derived from that are shown in figure 5. In order to facilitate the comparison between upper and lower surface the quasi-steady pressures at the upper surface are plotted with a reversed sign (Fig. 5.II). The agreement between the measured quasi-steady pressures and the prediction of thin airfoil theory is reasonable. The largest deviations show up over the rear part of the airfoil, where the measured data are below the calculated curve. Near the leading edge the measured pressures on the upper surface are larger than predicted by the theory and also larger than the values measured on the lower surface. As will be discussed later (chapter 4) the differences observed have to be attributed to the combined effect of airfoil thickness (plus incidence) and the boundary layer. The first effect dominates on the front part of the airfoil, while the boundary layer effect is more pronounced on the rear part.

A comparison between the unsteady pressures measured on the upper surface of the oscillating airfoil and the corresponding results of thin airfoil theory (Fig. 6) shows similar differences as observed in quasi-steady flow. In general the agreement between theory and experiment is reasonable. Further it can be noted that there is a very satisfactory agreement between the unsteady pressures measured directly with the in situ transducers and the pressures obtained via the pressure tubes.

3.2.2 Transonic flow with shock (condition B)

The next example concerns oscillations of the airfoil about the off-design condition B (Fig. 4). In this condition, being typical for "classical" transonic flow, the upper surface carries a supersonic region extending to about 50 per cent of the chord, which is terminated by a relatively strong shock wave. As shown in figure 7.I a change in incidence of 1 degree results in a shift of the steady shock position of about 10 per cent of the chord. The flow along the lower surface remains subcritical.

From the corresponding quasi-steady pressure distributions (Fig. 7.II) it can be deduced that along the upper surface the pressure is dominated by the effect of the shock displacement, generating a high pressure peak, which of course cannot be predicted by thin airfoil theory. The quasi-steady pressure distribution on the subsonic lower surface is predicted reasonably well.

Unsteady pressure distributions on the upper surface are presented in figure 8 for three different frequencies. These results also show the dominant effect of the pressure peak due to the moving shock wave. It is noted that this pressure peak shifts from the real part of the pressure distribution to the imaginary part with increasing frequency. This is the result of the increased phase lag of the periodical shock motion relative to the motion of the airfoil, a phenomenon to be discussed in more detail in chapter 3.4.1.

By representing the unsteady pressure distributions in terms of magnitude and phase angle (Fig. 9) it further can be shown that the width and the height of the pressure peak associated with the periodical motion of the shock wave decreases as the frequency is increased. This is caused by the decrease of the amplitude of the shock motion with increasing frequency (see also chapter 3.4.1). Concerning the phase curves in figure 9 it should be noted that the measurements show a jump of about 180 degrees just downstream of the mean position of the shock wave. This jump is present already in quasi-steady flow and thus is not a dynamic effect.

From the comparison of the measured pressure distributions with the distributions calculated with thin airfoil theory (Figs. 8 and 9) it is evident that, as far as the upper surface is concerned, this theory is not applicable.

3.2.3 The "shock-free" design condition (condition C)

Of special interest is the unsteady behaviour of the airfoil near its "shock-free" design condition (condition C in figure 4). As shown in figure 10.I a variation in incidence of 0.5 degree about the design point leads to a considerable change of the steady pressure distribution along the upper surface. In particular in the supersonic region, ranging from about 3 per cent to about 65 per cent of the chord the shape of the pressure distribution changes considerably. Further away from the design condition a (weak) shock wave shows up. At the lower surface the steady pressure distribution changes less drastically. Noteworthy is that along the lower surface the velocity becomes slightly supercritical, but still without shock formation.

The changes in steady distribution result in a quasi-steady distribution as given in figure 10.II. On the upper surface a wide bulge occurs, which is caused by the drastic change of the pressure distribution in the supersonic region. Most probably this wide bulge is a feature typical of this type of "shock-free" airfoil, characterized by a relative blunt nose and an extensive region of supersonic flow. A comparison between the measured quasi-steady distribution and the curve determined with thin airfoil theory shows that the prediction for the upper surface is quite useless. For the lower side, where the flow remains almost subcritical, the differences between theory and experiment is considerably smaller.

A series of fully unsteady pressure distributions along the upper surface in terms of magnitude and phase angle is given in figure 11. One easily recognizes in the magnitude curves the large contributions associated with the changes in the shape of the pressure distribution in the supersonic region on the front part of the airfoil. In addition a small peak occurs at about 65 per cent of the chord, caused by the periodical formation of a weak shock in this region (see figure 12). This peak grows larger with increasing frequency as a result of the increased strength of the shock wave. At the same time the bulge on the front part decreases with frequency and the unsteady pressure distribution shows a tendency to change in a direction towards the pressure distributions found for flow condition B.

The phase curves shown in figure 11 behave very regular up to about 60 per cent of the chord. Then a jump in phase angle of about 180 degrees occurs, which can be attributed to the presence of the shock wave.

Finally a comparison of the measured unsteady pressure distributions with thin airfoil theory confirms what could be concluded already on the basis of the quasi-steady data: for these types of mixed flow one has to rely on other prediction methods.

3.3 Unsteady aerodynamic derivatives

Of prime concern to the aeroelastician of course are the overall unsteady aerodynamic airloads. For this reason the unsteady aerodynamic coefficients, obtained by unwise integration of the measured unsteady pressure distributions, have been collected in figures 13-15, for the characteristic flow conditions A, B and C, respectively. For reference purposes the results according to thin airfoil theory are given as well.

The agreement between the theoretical and experimental pressure distributions for the subsonic flow condition A (see chapter 3.2.1) is reflected also in the curves of figure 13, representing the unsteady aerodynamic derivatives as a function of reduced frequency. The largest deviations, occurring in the real part of both the normal force and the moment derivative, can be attributed to the differences in the pressure distributions, which do exist already in quasi-steady flow (Fig. 5).

For the transonic flow condition B (see figure 14) the differences between theory and experiment are considerably larger than in the preceding fully subsonic example. This is true also for the unsteady derivatives in the "shock-free" design condition C (Fig. 15). A comparison between figures 14 and 15 learns that for the design condition the deviations from thin airfoil theory are of the same order of magnitude as for the "classical" transonic flow condition B.

The behaviour of the aerodynamic coefficients in a transonic flow with shock wave can be correlated qualitatively with the presence of the dominant pressure peak generated by the oscillation of the shock. As indicated schematically in figure 16 (representing for instance the results of flow condition B), the pressure peak associated with the shock wave is responsible for a shift in unsteady lift and moment indicated by a 1. At small reduced frequencies the real part of the normal force derivative, k_a , is larger than predicted by theory. As the frequency increases, the real part decreases faster than the curve for thin airfoil theory, while the imaginary part becomes much more negative than predicted. This behaviour is correlated with the shift of the pressure peak due to the shock from the real part to the imaginary part of the unsteady pressure distribution, as has been shown in figure 8 (see also section 3.2.2).

The same phenomenon is responsible for the change indicated by 1, in the moment derivative, m_a . The remaining part of the deviation in the moment derivative is caused by the circumstance that the mentioned pressure peak is located downstream of the quarter chord point, thus giving rise to a rearward shift of the aerodynamic centre. For the present example this shift, expressed as

$$\frac{\Delta x}{c} = \frac{1}{2} \frac{\Delta m_a}{k_a}$$

can be estimated roughly at 5 per cent of the chord.

In the figures 13-15 results are given for the airfoil with and without transition strip. For flow conditions A and B no significant difference is observed. However, in the delicate "shock-free" design condition C the flow is more susceptible to disturbances over the front part of the airfoil and thus more sensitive to the presence of the strip. For a more detailed account on this sensitivity reference is made to reference 7.

Further it should be remarked here that the measured data are given without tunnel wall correction, since reliable methods to determine this effect in unsteady wind tunnel tests are not yet available. An estimate of the amount of wall interference involved in the present tests will be given in chapter 4 on the basis of some quasi-steady flow calculations.

3.4 Remarks on the unsteady shock wave motion

3.4.1 Effect of frequency

With the help of optical flow studies additional information is obtained about the periodical motion of the shock waves in flow condition B. From figure 17, giving the time histories of the shock displacement for different frequencies, it follows that the shock wave performs nearly sinusoidal motions (similar to the type A motion described in reference 8). Further the phase lag of the shock motion relative to the airfoil motion increases with frequency, while the amplitude of the shock motion decreases. The latter corresponds very well with the observations mentioned earlier concerning the contribution of the moving shock wave to the unsteady pressure distributions (see Figs. 8 and 9).

A closer examination of the phase lag of the shock motion with respect to the airfoil motion (Fig. 18) learns that an almost linear relationship exists between frequency and phase lag. This implies that there is a constant time lag between the motion of the airfoil and the shock wave motion. In relation to this it is of interest to recall the investigation of Erickson and Stephenson (Ref. 9) who have found that a fixed relation seems to exist between the phase lag of the shock motion and the time required for a pressure impulse to travel from the trailing edge to the shock wave. Indeed this travelling time seems to be a logical parameter for an airfoil with a large supersonic region terminated by a shock wave, because this is the time period after which major changes in flow condition, namely changes in flow direction at the trailing edge (Kutta condition) can be felt by the shock wave (Fig. 19).

The time required to forward information from the trailing edge to the shock wave amounts

$$\Delta t = \int_{x=c}^{x_s} \frac{dx}{(1-M_{loc})a_{loc}}$$

with M_{loc} being the local Mach number and a_{loc} the local velocity of sound. Due to the gradient in Mach number normal to the airfoil surface the acoustic waves propagate along paths away from the airfoil. Therefore the propagation speed in upstream direction will be some average between the value of $(1-M_{loc})a_{loc}$ near the airfoil surface and the free stream value. To account for this effect the following value of the local Mach number has been introduced:

$$M_{loc} = R [M_{loc}(\text{at the surface}) - M_\infty] + M_\infty$$

with R being a relaxation factor, which has a value between 0 and 1.0. For $R=0.7$ an excellent agreement is obtained between the travel time of the "Kutta waves" and the corresponding phase lag of the shock motion, as is demonstrated in Figure 18. This value of R agrees very well with the relaxation factor applied in the modified Loubier lattice method of NLR (see Roos, Ref. 10), in which in a semi-empirical way a local Mach number correction is introduced. In this method also the factor R is used to account for the gradients in Mach number normal to the airfoil surface.

3.4.2 Linearity of the unsteady loads

The local pressures in points of the airfoil located within the trajectory of the oscillating shock wave show a strong nonlinear behaviour, caused by the periodical passage of the shock and the accompanying pressure jump. From the time registrations of the unsteady pressures and the resulting overall loads (see example of figure 20) it can be noted, however, that in spite of these local non-linearities the resulting unsteady lift varies almost sinusoidal. The overall moment shows irregularities, but its amplitude is very small and strongly amplified. These findings correlate very well with the experiences of Magnus and Yoshihara (Ref. 11), Laval (Ref. 12) and Krupp and Murman (Ref. 13), who in their calculated examples also observed an almost linear behaviour of the overall aerodynamic derivatives, in spite of the presence of an oscillating shock wave.

This phenomenon can be made plausible as follows. In flow patterns with a well developed shock wave it has been observed that the shock motion takes place almost sinusoidal and that the amplitude of the shock motion is almost proportional to the amplitude of the sinusoidal motion of the airfoil (see for instance figure 21). This makes it possible to introduce the schematized model of figure 22, in which the change in pressure in a fixed point A is considered, while the shock wave performs a sinusoidal motion of amplitude x_s .

As derived in reference 8 the local shock strength in point A, located within the shock trajectory, can be written as:

$$(p_2 - p_1)_{x_a} = (p_2 - p_1)_{x_s} \cdot u(x_a - x_0 e^{i\omega t}) + \Delta p(\omega, M_1, \frac{\partial M_1}{\partial x}) \cdot x_0 e^{i\omega t}$$

Here $u(x_a - x_0 e^{i\omega t})$ denotes the unit step function and Δp the variation in shock strength during the shock wave motion. For strong shock waves and small amplitude motions the last term in the above expression can be discarded relative to $(p_2 - p_1)_{x_s}$. When $(p_2 - p_1)_{x_s}$ is described as a function of time a block type signal occurs (see figure 22), of which the Fourier decomposition yields:

$$f(x_a) = \left[(p_2 - p_1)_{x_s} - (p_2 - p_1)_{x_s} \frac{1}{\pi} \arccos \frac{x_a}{x_0} \right] - (p_2 - p_1)_{x_s} \left[\frac{2}{\pi} \sin(\arccos \frac{x_a}{x_0}) \cos \omega t + \frac{1}{\pi} \sin(2 \arccos \frac{x_a}{x_0}) \cos 2\omega t + \frac{2}{3\pi} \sin(3 \arccos \frac{x_a}{x_0}) \cos 3\omega t + \dots \right]$$

The corresponding distribution of the first four Fourier components along the trajectory of the shock motion are shown in figure 23. From the distribution of the mean steady value it follows that, due to the oscillatory motion of the shock wave, the jump in the steady pressure distribution is spread out over the shock trajectory. The distribution of the component with the same frequency as the airfoil motion shows a maximum of $2/\pi$ times the steady pressure jump $(p_2 - p_1)_{x_s}$.

Integration of the various components over the shock trajectory to obtain the contribution to the overall unsteady lift and moment learns that the lift contains only a contribution of the fundamental frequency. The resulting unsteady moment also contains a term $(p_2 - p_1)_{x_s} \cdot x_0^2 \cdot \cos 2\omega t$. So it can be expected that the second harmonic shows up first in the unsteady moment.

From the considerations given above it follows also that measuring the first Fourier component of the pressure signals, as is done in the present tests via the tubing system, gives by chordwise integration a correct value of the unsteady lift. As far as the moment is concerned the second harmonic of order x_0^2 can not be distinguished.

4. EXPECTED CAPABILITY OF THE NEW CALCULATION METHODS

In the preceding analysis of the experimental data the results of thin airfoil theory have been added as a reference for two reasons. Firstly these results serve as a simple basis for the distinction of the typical transonic phenomena and secondly, linear lifting surface theory is widely used in aerodynamic applications. As long as the flow is moderately subsonic thin airfoil theory has proven to be a rather adequate tool indeed. However, from the preceding discussions it is apparent, that calculation methods for transonic flow should include the effect of airfoil thickness, incidence and - if shock waves are present - also the effects of the periodical shock wave motion.

In recent years considerable progress has been achieved in solving the non linear equations for unsteady transonic flow (reviews on the current status are given in references 14-20). With one exception (Ref. 21) all new calculation methods are dealing with inviscid flow. In order to get an impression about the improvements one might expect from these methods some comparisons will be presented between theory and experiment for the NLR 7301 airfoil. At this moment the comparison is limited to quasi-steady flow, but in the near future comparative studies will be performed also for fully unsteady flow.

Considering first the quasi-steady case has the advantage that a reasonable estimate can be given of the effect of the boundary layer, by using an existing method for steady transonic flow, which includes the displacement effect of the boundary layer (Bauer, Korn, Garabedian and Jameson (Ref. 22)). Further for quasi-steady flow a rather accurate estimate can be given of the severity of interference from the plotted tunnel walls, a situation which is not yet reached for unsteady measurements.

Mach number as in the experiments, but for an incidence α_0 , which includes the correction for wall interference. For the NLR Pilot tunnel this correction has been established to be $\Delta\alpha = 0.01$.

$$\Delta\alpha = C_l / C_f$$

where C_l is steady lift coefficient and C_f a coefficient, depending on the free stream Mach number (Fig. 24).

4.1 Fully subsonic flow (condition A)

Calculated and measured results for the airfoil in the subsonic flow condition A are shown in figure 25. Figure 25.I reveals a significant effect of the boundary layer in the steady mean position of the airfoil. The corresponding quasi-steady results (Fig. 25.II) demonstrate that the deviations of the test results from thin airfoil theory, as discussed in chapter 3.2.1, are due to the combined effects of thickness, incidence and viscosity. The effect of thickness and incidence dominates on the front part of the airfoil and the effect of viscosity towards the rear.

For the quasi-steady results the wall correction has been applied on the measured data, since this effect can be translated simply in an additional change of effective incidence due to the change in lift. This additional change has to be subtracted from the geometrical change in incidence. From the results in figure 25.II it can be noted that the tunnel walls have a considerable effect.

4.2 Transonic flow with shock wave (condition B)

The second example deals with the transonic flow condition B (Fig. 4). In steady flow (Fig. 26.I) viscosity again has a large effect, in particular on the location of the shock wave. The importance of inserting boundary layer effects is reflected also in the quasi-steady results (Fig. 26.II). On the upper surface a considerably improved prediction is obtained, when thickness and boundary layer effects are considered simultaneously. Especially the location of the high pressure peak resulting from the shift in shock position is predicted much better.

The improvements achieved can be observed also in the quasi-steady aerodynamic coefficients, collected in table 1. For instance these data show that at $M_\infty = 0.7$ thickness and incidence are responsible for an increase of the thin airfoil value of the normal force coefficient, k_α , of more than 50 per cent. The inclusion of the boundary-layer leads to a decrease of the order of 35 per cent, as can be observed by comparing the results with and without boundary layer, both obtained with the non-conservative calculation scheme (the conservative scheme, which guarantees the best numerical solution of the transonic flow equations did not converge for inviscid flow so this value could not be added). From the last two columns it follows that the tunnel wall effect in the present tests is considerable and accounts to about 25 per cent. At $M_\infty = 0.5$ the effects mentioned are less than at transonic speed, but still significant.

TABLE 1

Quasi-steady aerodynamic derivatives (NLR 7301 airfoil)

				Thin airfoil theory		Inviscid theory + thickness		Inviscid theory + thickness + boundary layer		Inviscid theory + thickness + boundary layer + wall interference		Experiment	
						Non-conservative F-D scheme		Non-conservative F-D scheme		Conservative F-D scheme		Conservative F-D scheme	
M_x	α_o	k_α	m_α	k_α	m_α	k_α	m_α	k_α	m_α	k_α	m_α	k_α	m_α
0.5	0.85°	2.31	0	2.73	0.043	2.53	-0.036	2.53	-0.036	2.22	-0.032	2.18	-0.090
0.7	3.00°	2.80	0	4.24	0.11	3.21	0.00	3.92	-0.22	3.23	-0.18	3.20	-0.34

F-D= Finite difference

From the examples discussed so far a good impression is obtained about the improvements which can be expected at most from the inclusion of thickness and incidence theories. Clearly the inclusion of these effects is an important step forward, which on itself, however, does not lead to improved predictions. A genuine improvement in this respect can be achieved only if the second step is made also, i.e. the inclusion of boundary layer effects.

A weak point in the considerations given above is seemingly that the examples deal with a relatively low Reynolds number ($\sim 2 \cdot 10^6$). However, similar calculations for higher values of this parameter (up to $30 \cdot 10^6$, with fixed transition point) do not exhibit a significant sensitivity to Reynolds number changes. This seems to indicate that under full scale conditions the effect of viscosity remains of the same order of magnitude as shown here.

4.3 The "shock-free" design condition (condition C)

To conclude the evaluation of the capability of advanced theories on the basis of quasi-steady flow the "shock-free" flow condition C will be considered. For this purpose a comparison is made between results calculated for the theoretical "shock-free" design condition and results measured for condition at which "shock-free" flow is obtained in the wind tunnel. In this way the circumstance that the experimental design condition (i.e. Mach number and incidence) differs from the inviscid theoretical design condition can be discarded, assuring that both theory and experiment deal with the carefully balanced condition of "shock-free" flow.

The steady pressure distributions computed for incidences at and around the design condition (Fig. 27.I) exhibit in the supersonic region at the upper surface the same marked changes in the shape of the pressure distribution as observed in the measurements (Fig. 10). The lower surface be-

thin airfoil theory. The typical hump character of the distribution on the upper surface is predicted reasonably well and also the prediction for the lower surface is improved. This justifies the expectation that methods based on inviscid theory are able to predict at least qualitatively the main characteristics of the unsteady flow for oscillations around the "shock-free" design condition.

5. CONCLUDING REMARKS

From the preceding evaluation it is apparent that the inclusion of airfoil thickness, incidence and transonic shock motions in inviscid flow calculations leads to an improvement of the theoretical predictions in an at least qualitative sense. In quantitative sense a large discrepancy with the real flow will remain as a result of the boundary layer, which to a large extent determines the final location of the shock and by that the overall unsteady airloads. However, as the modelling of unsteady boundary layers is only in its first phase (for a review of the present status reference is made to Ref. 3) it is unlikely that in the near future sophisticated calculation methods will become available for this purpose. Therefore in the coming period an engineering type of approach has to be followed. In this respect the ideas developed by Magnus and Yoshinara (Ref. 11) deserve attention, since their relatively simple "viscous ramp" model lends itself for easy implementation in inviscid calculation methods.

From a computational point of view small perturbation methods are very attractive. It should be investigated, therefore, what the limits of such methods are, in particular when applied to thick supercritical airfoils of the type as the one considered in this paper. In this respect it should be noted that the impressions given in the preceding chapter about the improvements attainable with the new calculation methods are based on solutions of the full potential equation, without assuming small perturbations.

Further from the considerations of the quasi-steady results of the NLR 7301 airfoil it has become clear that in order to improve the reliability of comparisons between theory and wind tunnel data there is an urgent need for methods to assess the amount of wall interference in unsteady experiments in transonic test sections with slotted or porous walls. Finally the insight with respect to the effect of Reynolds number, being already a crucial parameter in steady transonic flow, should be increased by performing tests in a high Reynolds number test facility.

6. ACKNOWLEDGEMENT

The experimental data presented in this paper have been obtained in an investigation carried out in collaboration with Fokker-VFW under contract with the Netherlands Agency for Aerospace Programs (NIVR). The authors are indebted to the NIVR and Fokker-VFW for the permission to use this material.

7. REFERENCES

- 1 Boerstoeel, J.W. and Huizing, G.H. Transonic shock-free aerofoil design by an analytic hodograph method. *Journal of Aircraft*, 12 No. 9, pp 730-736, 1975.
- 2 Boerstoeel, J.W. Review of the application of hodograph theory to transonic aerofoil design and theoretical and experimental analysis of shock-free aerofoils. *Symposium Transsonicum II*, Göttingen, Sept. 1975.
- 3 Rohne, B. Data report of a wind tunnel investigation on airfoil section NLR 7301. NLR report TR 74049 G, 1974.
- 4 Ewaaneveld, J. Aerodynamic characteristics of the supercritical shock-free airfoil section NLR 7301. NLR report TR 76052 G, 1976.
- 5 Poestkoze, P. Hydraulic test rig for oscillating wind tunnel models. NLR report MP 76020 U, 1976.
- 6 - Facilities and Equipment at NLR
- 7 Tijdeman, H. Investigations of the transonic flow around oscillating airfoils. Dissertation Technical University Delft (to be published).
- 8 Tijdeman, H. On the motion of shock waves on an airfoil with oscillating flap. *ISUTAN Symposium Transsonicum II*, Göttingen, Sept. 1975. eds. Sawatzsch, K and Rues, D Springer Verlag, Berlin 1976. (see also NLR report TR 75038 U).
- 9 Erickson, R.L. and Stephenson, G.L. A suggested method of analyzing for transonic flutter of control surfaces based on experimental evidence. *NACA RM A7F 30*, 1947.
- 10 Roos, P. Application of Panel Methods for unsteady flow. NLR report TR 76010 U, 1976.
- 11 Magnus, R.J. and Yoshinara, H. Calculations of transonic flow over an oscillating airfoil. *AIAA paper 75-28*, 13th Aerospace Sciences Meeting Pasadena, 1975.
- 12 Laval, P. Calcul de l'écoulement instationnaire transsonique autour d'un profil oscillant par une méthode à pas fractionnaires. *ONERA TR No. 1075-115*, 1975.

- 13 Krupp, J.A. and Cole, J.D. Studies in Transonic Flow IV
Unsteady Transonic Flow
UCLA-Eng-76104, Oct. 1976
- 14 Bland, S.R. Recent advances and concepts in unsteady aerodynamic theory.
NASA SP-347: Aerodynamic analysis requiring advanced
computing, March 1975, pp 1305-1326.
- 15 Tijdeman, H. High subsonic and transonic effects in unsteady aerodynamics
part of AGARD report No. 636, 1976.
- 16 Stahara, J.R. and Spreiter, S.S. Unsteady Transonic Aerodynamics - An aeronautical Challenge
Symposium on Unsteady Aerodynamics.
ed. Kinney, R.B., Univ. of Tucson, 1975, pp 553-581.
- 17 Landahl, M.T. Some developments in unsteady transonic flow research.
IUTAM Symposium Transsonicum II, Göttingen, Sept. 1975.
eds. Oswatitsch, K and Rues, D; Springer Verlag, Berlin, 1976.
- 18 Ballhaus, W.F. Some recent progress in transonic flow computations.
Lecture series No. 87 on Computational Fluid Dynamics, von
Karman institute, Rhode-St-Genese, Belgium, March 1976.
- 19 Wu, J.M. and Moulden, T.H. A survey of transonic aerodynamics.
AIAA paper 76-326; AIAA 9th Fluid and Plasma Dynamic Confe-
rence, San Diego, Ca., July 1976.
- 20 Mc Croskey, W.J. Some current research in Unsteady Fluid Dynamics.
Journal of Fluids Engineering, Vol. 99, No. 1, March 1977.
- 21 Magnus, R. and Yoshinara, H. The transonic oscillating flap.
AIAA paper 76-327; AIAA 9th Fluid and Plasma Dynamic Confe-
rence, San Diego, July 1976.
- 22 Bauer, F., Garabedian, P., Korn, D. and Jameson, A. Supercritical wing sections II.
Lecture notes on Economics and Math. Systems No. 108.
Springer Verlag, 1975.
- 23 Smith, J. Values of the wall interference corrections for the NLR
Pilot tunnel with 10 % open slotted test section.
NLR int. report AC 74-01, 1974.

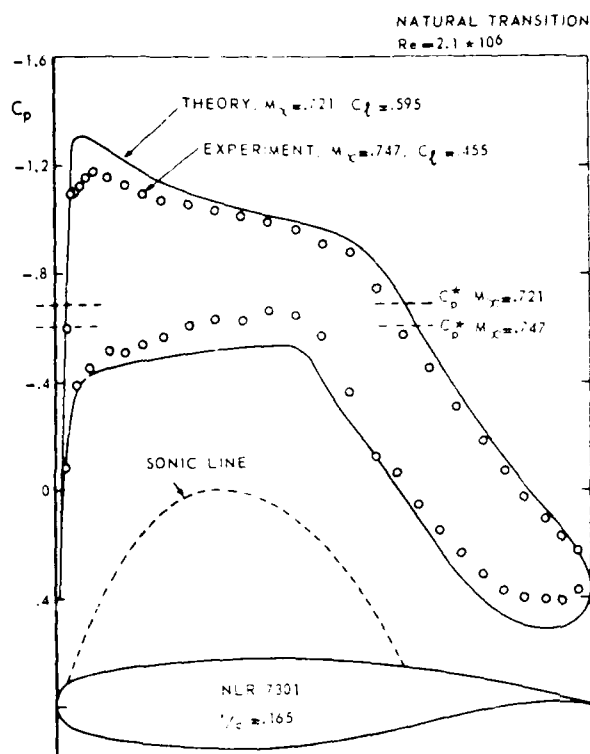


Fig. 1 Theoretical and experimental shock-free pressure distributions of the NLR 7301 airfoil (Reproduced from [4])

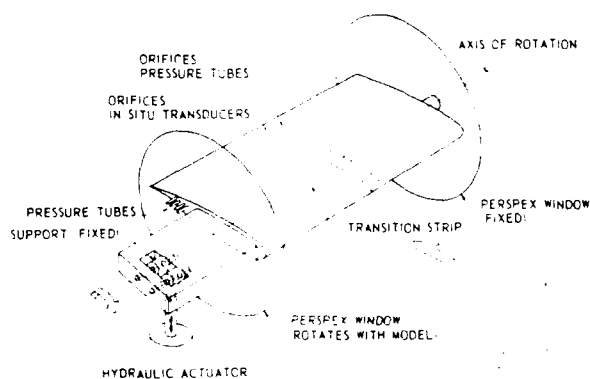
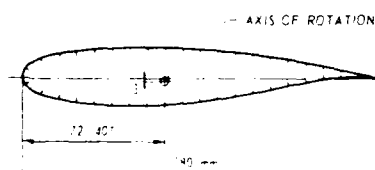


Fig. 2 Schematic view of test set up



PRESSURE ORIFICES TUBING SYSTEM BOTH UPPER AND LOWER SURFACE			
NO. 1	$x/c = .01$	NO. 11	$x/c = .50$
2	.05	12	.55
3	.10	13	.60
4	.15	14	.65
5	.20	15	.70
6	.25	16	.75
7	.30	17	.80
8	.35	18	.85
9	.40	19	.90
10	.45	20	.95

IN SITU TRANSDUCERS UPPER SURFACE ONLY			
NO. 1	$x/c = .04$	NO. 11	$x/c = .70$
2	.10	12	.80
3	.19	13	.88
4	.28		
5	.34		
6	.40		
7	.46		
8	.52		
9	.58		
10	.64		

LIFT COEFFICIENT

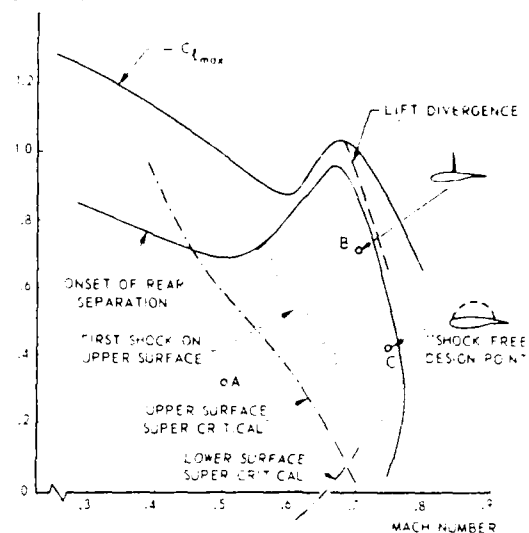


Fig. 4 C_L - M plane for NLR 7301 airfoil ($r/c = 0.165$)

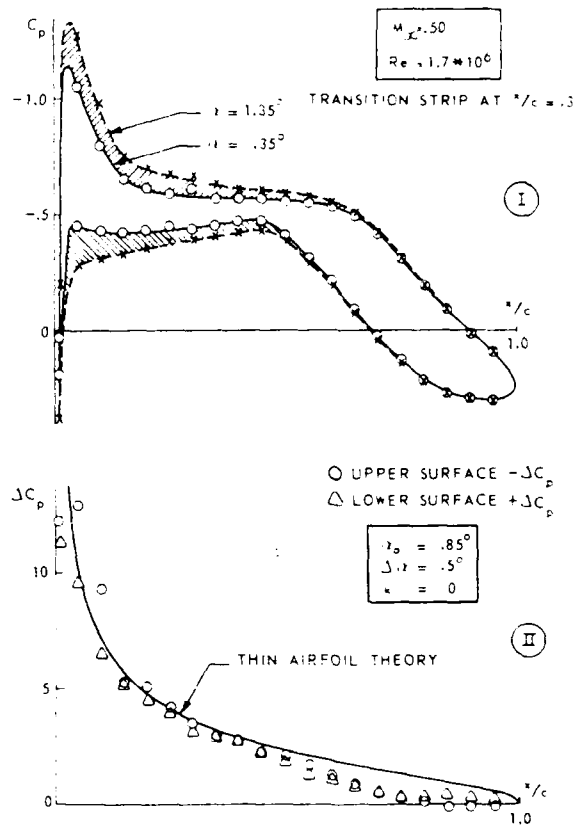
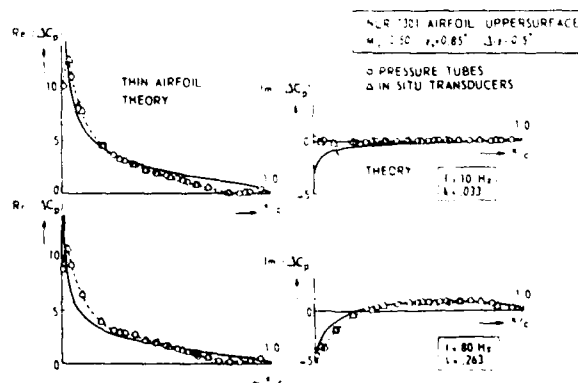


Fig. 5 Steady and quasi-steady pressure distributions on NLR 7301 airfoil at subsonic speed (Condition A)



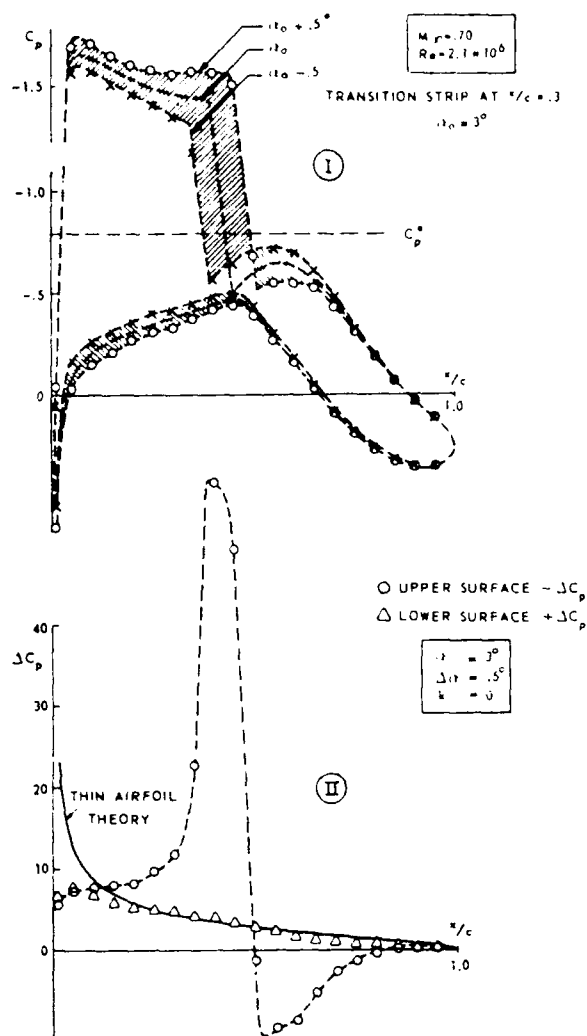


Fig. 7 Steady and quasi-steady pressure distributions on NLR 7301 airfoil in transonic flow with shock wave (Condition B)

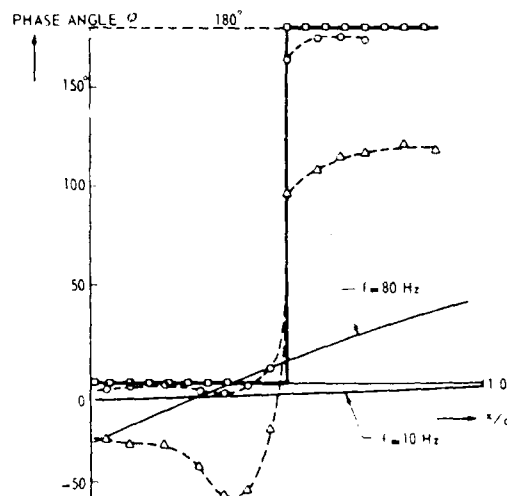
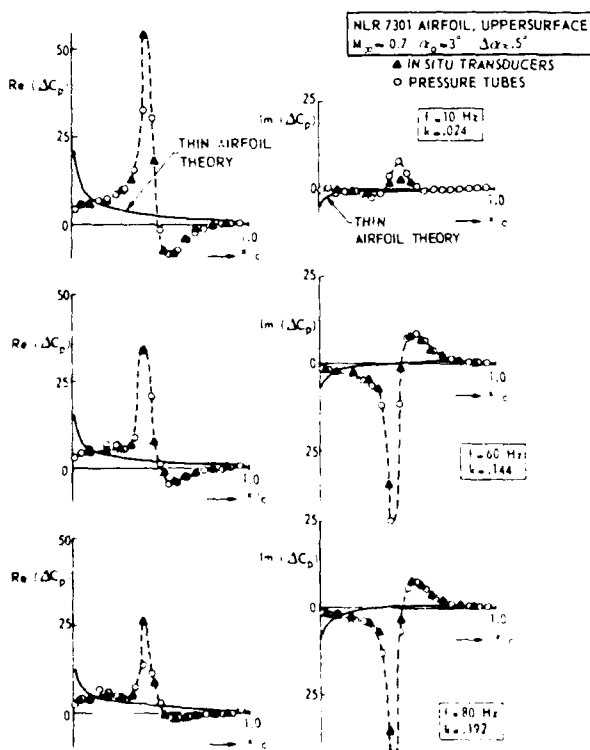
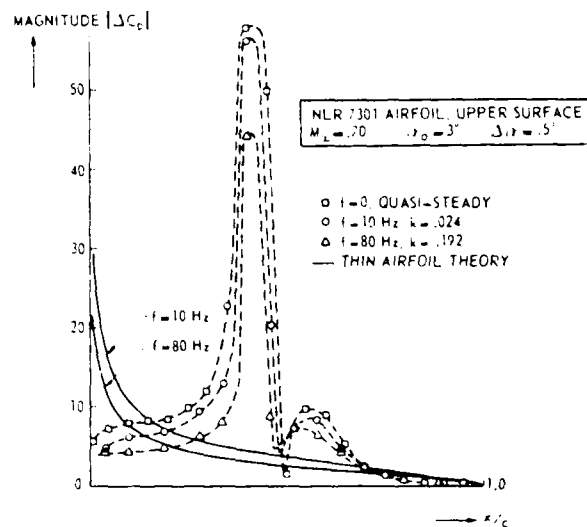


Fig. 9 Effect of a shock wave on the unsteady pressure distributions (Condition B)

Fig. 8 Development of unsteady pressure distributions with

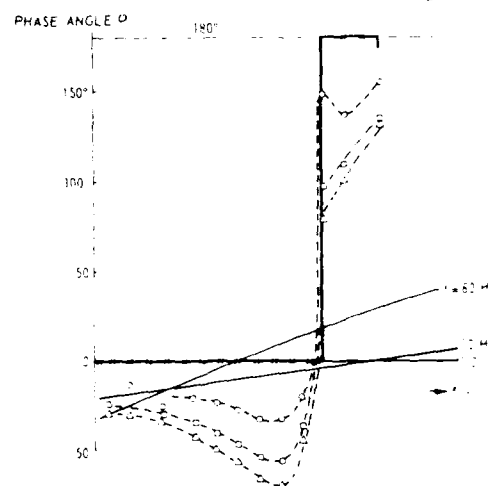
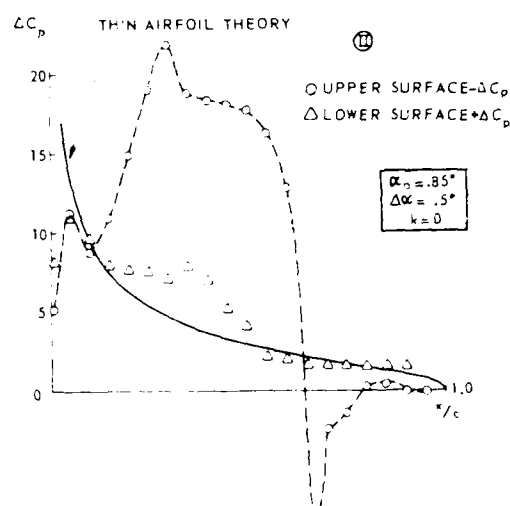
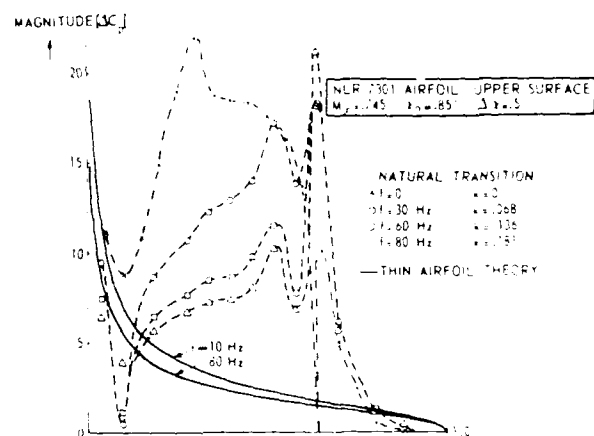
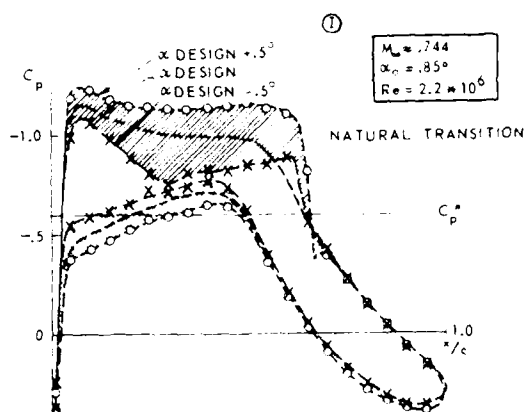


Fig. 10 Steady and quasi-steady pressure distributions on NLR 7301 airfoil around the design point (Condition C)

Fig. 11 Unsteady pressure distributions for the "shock-free" design condition (Condition C)



I MAXIMUM α

CONDITION C

$$M_\infty = .745$$

$$f = 60 \text{ Hz}$$

$$\alpha_0 = .85^\circ$$

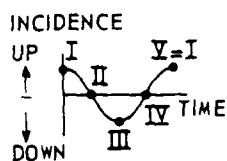
$$\Delta \alpha = .5^\circ$$



II



III MINIMUM α



IV

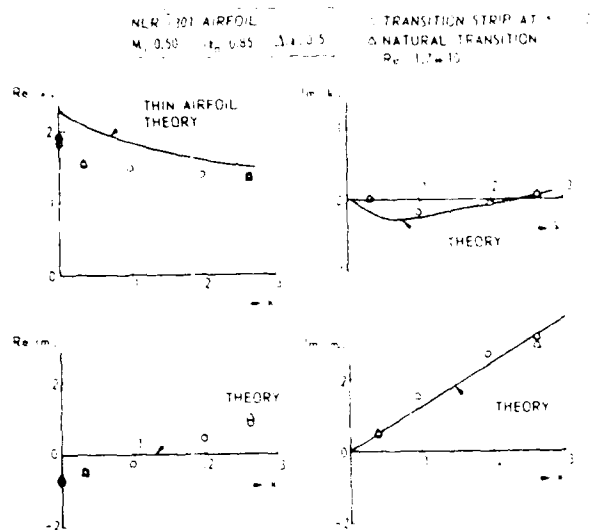


Fig. 13 Unsteady normal force and moment coefficients as a function of frequency in subsonic flow (Condition A)

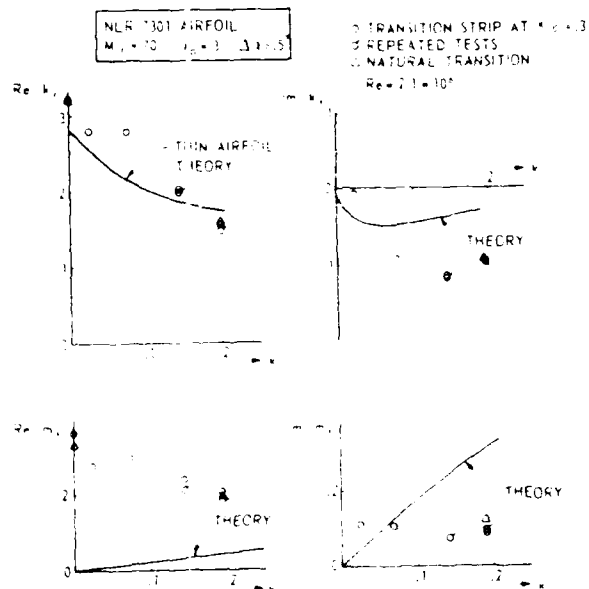


Fig. 14 Unsteady normal force and moment coefficients as a function of frequency (Condition B)

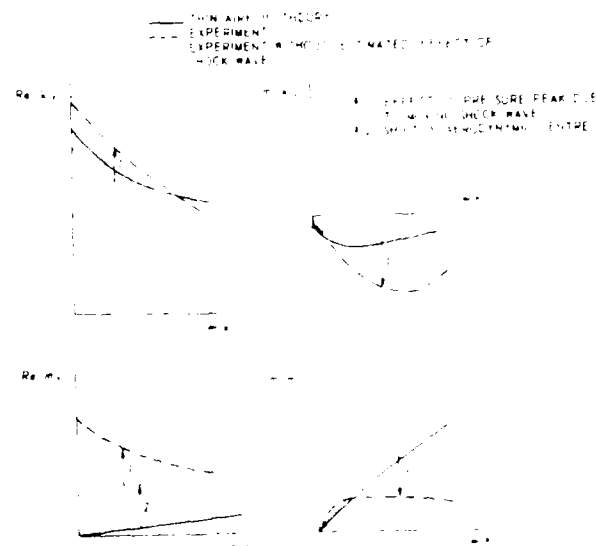
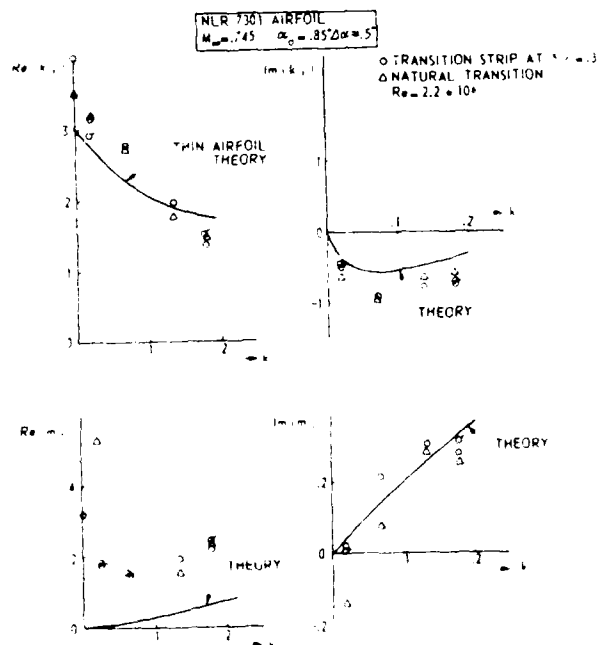


Fig. 16 Qualitative explanation of the effect of the oscillating shock wave on the unsteady aerodynamic coefficients

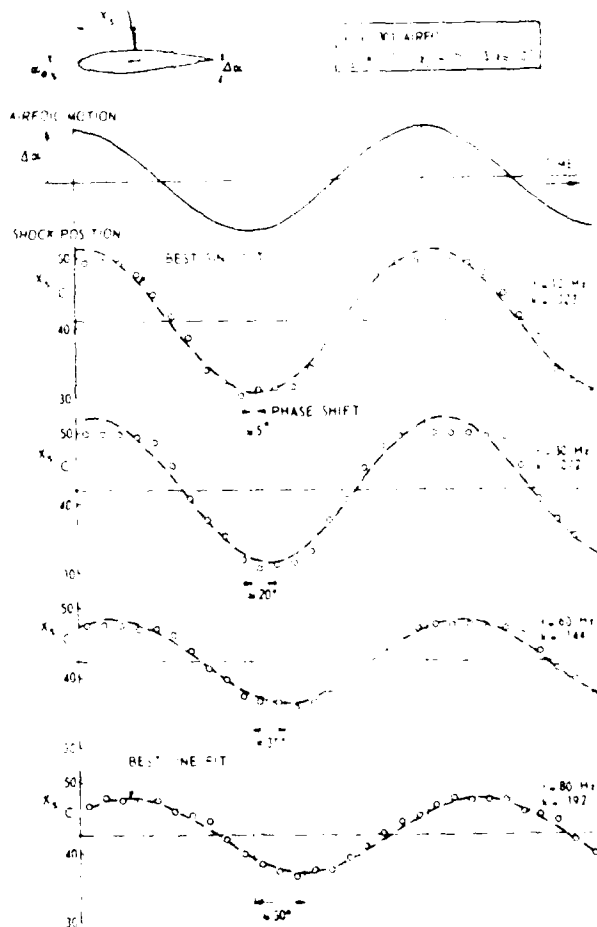


Fig. 17 Periodical shock wave position as a function of frequency (Condition C)

PHASE LAG IN SHOCK WAVE MOTION



AMPLITUDE OF SHOCK WAVE MOTION

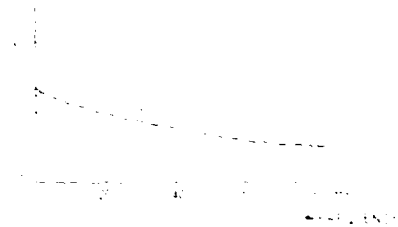


Fig. 15 Effect of frequency on the amplitude and phase lag of the periodic shock wave motion - Condition B



AIRFOIL MOTION

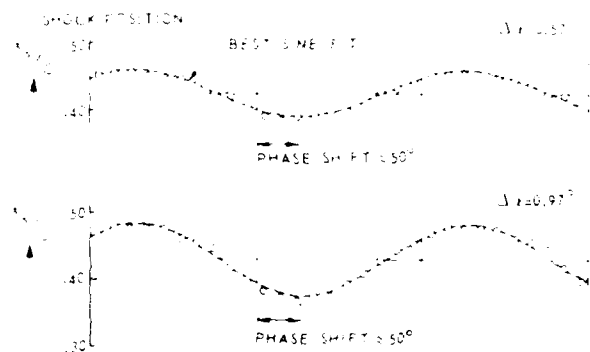


Fig. 21 Influence of amplitude of airfoil oscillation on shock wave motion - Condition B

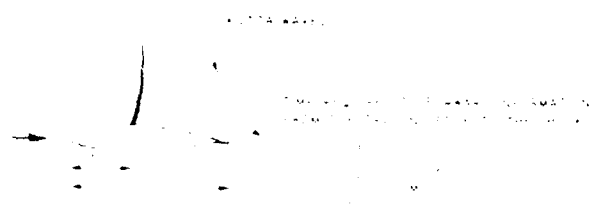
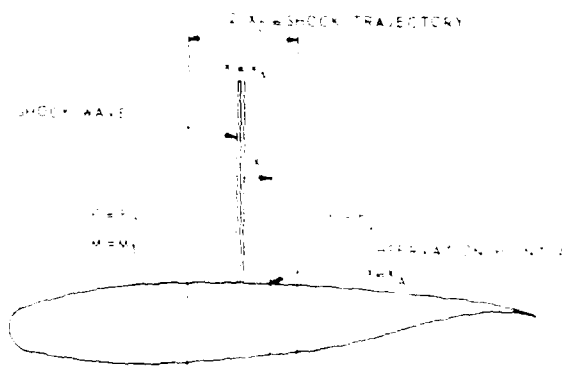


Fig. 17 The propagation of information from the trailing edge to the shock wave



SHOCK WAVE

SHOCK TRAJECTORY

SHOCK WAVE MOTION

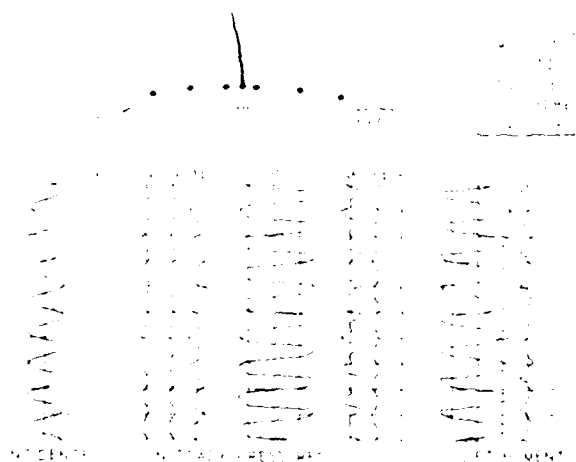


Fig. 20 Example of unsteady pressure signals in an axial flow with a shock wave

ASSEMBLED SHOCK DISPLACEMENT PRESSURE IN POINT A

Fig. 22 Contribution of a periodic moving shock wave to the pressure signal at a fixed observation point

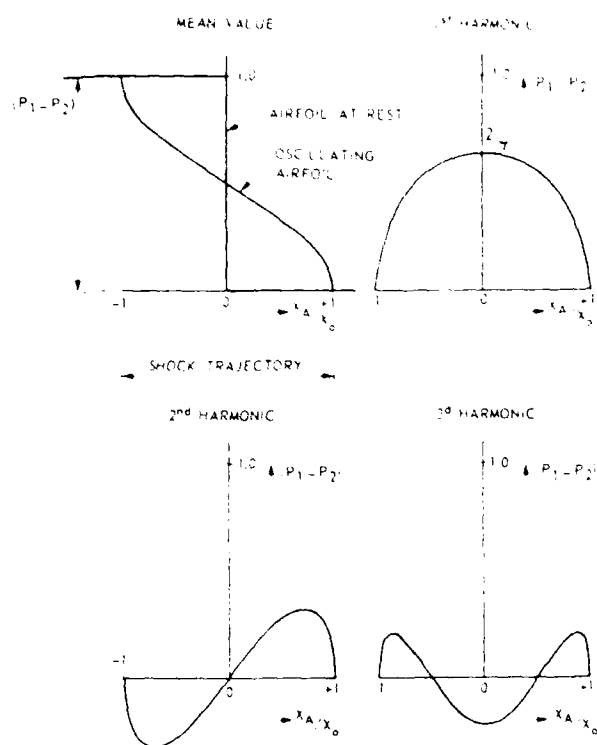


Fig. 23 Distribution of the first four Fourier components along the trajectory of the shock motion

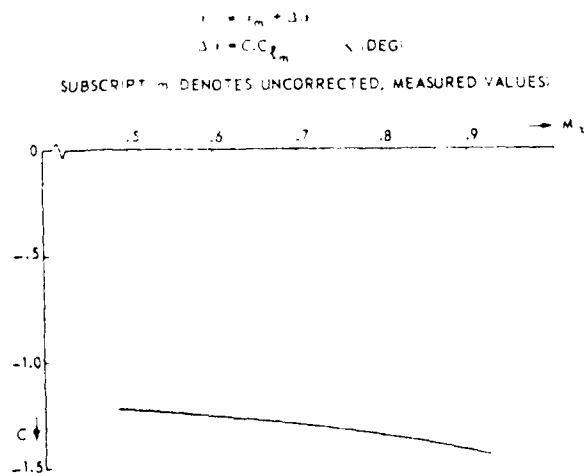


Fig. 24 Wall interference correction for the NLR P lot tunnel

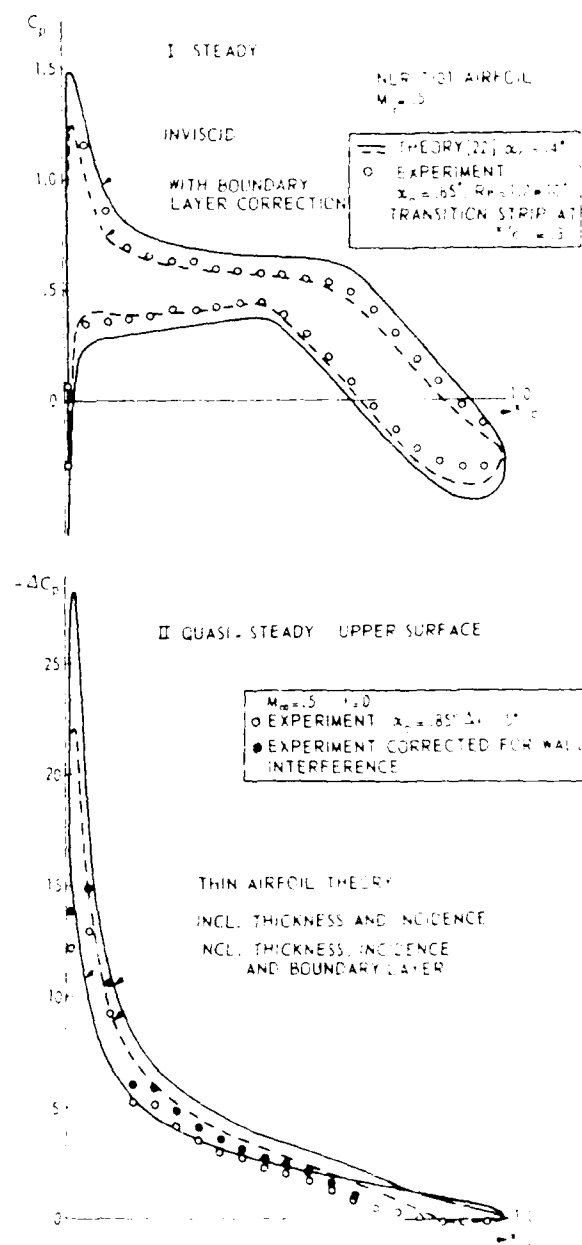


Fig. 25 Effect of thickness, incidence and boundary layer on the steady and quasi-steady pressure distributions in subsonic flow Condition A

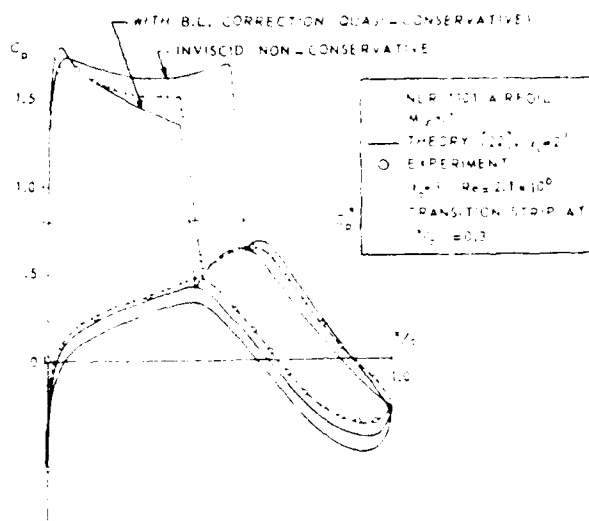


Fig. 26-I Steady pressure distributions in the mean position (Condition B)

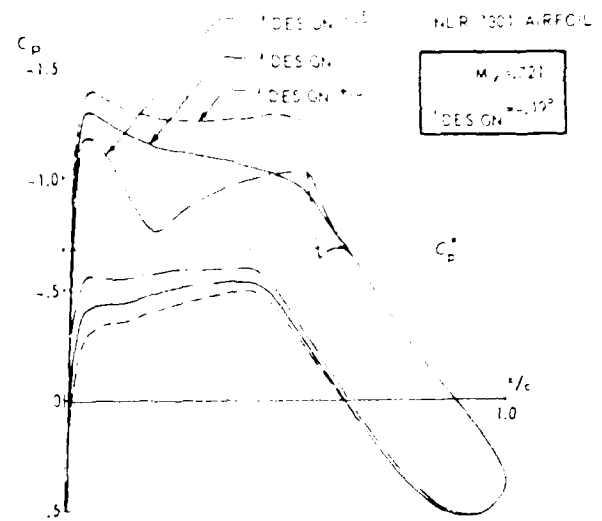


Fig. 27-I Calculated steady pressure distributions of and about the theoretical "shock-free" design condition (Non conservative scheme)

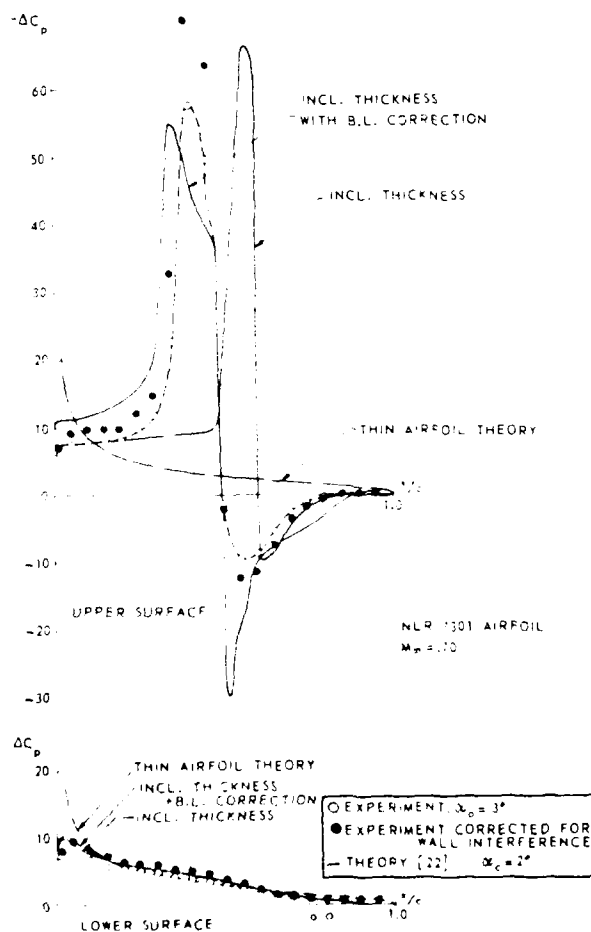


Fig. 26-II Quasi-steady pressure distributions (Condition B)

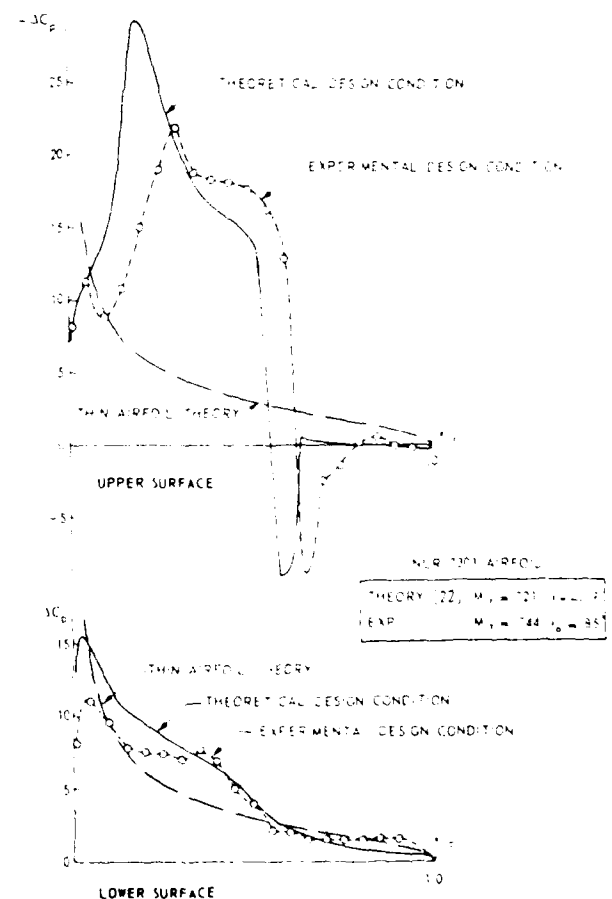


Fig. 27-II Quasi-steady pressure distributions for the theoretical "shock-free" design condition (Condition C)

END

FILMED

1-90

DTIC